JOURNAL OF GEOPHYSICAL RESEARCH, VOL. 101, NO. A9, PAGES 19,859-19,870, SEPTEMBER 1, 1996

A two-dimensional hybrid simulation of the magnetotail reconnection layer

Y. Lin

Physics Department, Auburn University, Auburn, Alabama

D. W. Swift

Geophysical Institute and Department of Physics, University of Alaska, Fairbanks

Abstract. Two-dimensional (2-D) hybrid simulations are carried out to study the structure of the reconnection layer in the distant magnetotail. In the simulation an initial current sheet separates the two lobes with antiparallel magnetic field components in the x direction. The current sheet normal is along the z direction. It is found that a leading bulge-like magnetic configuration and a trailing, quasi-steady reconnection layer are formed in a magnetic reconnection. If the duration of the reconnection is sufficiently long, the trailing reconnection layer will dominate the plasma outflow region. For the symmetric lobes with $B_y = 0$, two pairs of slow shocks are present in the quasi-steady reconnection layer. The slow shocks are expected to be fully developed at a sufficient distance from the X line, where the separation between the two shocks is greater than a few tens of the lobe ion inertial length. The Rankine-Hugoniot jump conditions of the slow shock are found to be better satisfied as the distance from the X line along the x axis increases. For the cases with $B_y \neq 0$ in the two lobes, two rotational discontinuity-like structures appear to develop in the reconnection layer. On the other hand, in the leading bulge region of a magnetic reconnection, no steady MHD discontinuities are found. Across the plasma sheet boundary layer the increase of the flow velocity appears to be much smaller than that predicted from the Rankine-Hugoniot jump conditions for a steady discontinuity, and the increase in the ion number density is much larger. In addition, a large increase in the parallel ion temperature is found in the plasma sheet boundary layer. The 2-D simulation results are also compared with the one-dimensional hybrid simulations for the Riemann problem associated with the magnetotail reconnection. It is found that the 2-D effects may lead to the presence of the non-switch-off slow shocks and thus the lack of coherent wave trains in slow shocks.

1. Introduction

In the Earth's magnetosphere, magnetic reconnection may take place at the magnetopause and in the magnetotail, where the magnetic field has a large shear [*Dungey*, 1961; *Sonnerup*, 1979; *Vasyliunas*, 1975; *Russell and Elphic*, 1978; *Hones*, 1979]. It is believed that through the magnetic reconnection process the solar wind mass, momentum, and energy can be efficiently transferred into the magnetosphere. A high-speed accelerated plasma flow is often present as a result of the magnetic reconnection. Similarly, reconnection in the magnetotail plasma sheet may lead to the earthward ejection of plasma flow.

Paper number 96JA01457
0148-0227/96/96JA-01457$09.00

In *Petschek*'s [1964] model of magnetic reconnection the reconnection configuration consists of three parts: an inflow region, an outflow region, and a small central diffusion region. The Petschek model describes the symmetric case with equal plasma density, equal magnetic field strength, and antiparallel magnetic fields on the two sides of the current layer. The outflow region contains two pairs of steady state slow shocks, across which the magnetic field decreases, the plasma density and temperature increase, and the plasma is accelerated. This model may be applied to a reconnection in the distant magnetotail, where the magnetic field and plasma density in the two lobes are highly symmetric and the reconnection may be quasi-stationary. On the other hand, at the dayside magnetopause, where the plasma and field are highly asymmetric across the current layer, a rotational discontinuity may be present in the outflow region of magnetic reconnection [*Levy et al.*, 1964; *Sonnerup et al.*, 1981; *Heyn et al.*, 1988; *Lin and Lee*, 1994]. The outflow region of magnetic reconnec-

tion which contains MHD discontinuities and shocks is referred to as the reconnection layer [*Heyn et al,*, 1988].

The Petschek type reconnection has been simulated by two-dimensional (2-D) MHD simulations, and slow shocks have been found in the outflow region [e.g., *Sato*, 1979; *Scholer and Roth*, 1987; *Shi and Lee*, 1990; *Yan et al.*, 1992]. The structure of the discontinuities in the reconnection layer, however, has not been studied in 2-D kinetic simulations.

Satellite observations in the distant magnetotail ($\sim$ 100 R_E) have shown the evidence of slow shocks in the lobe/plasma sheet boundary layer, namely, a decrease in magnetic field, an increase in plasma density and temperature, and a large accelerated flow in the central plasma sheet [e.g., *Feldman et al.*, 1984, 1985; *Smith et al.*, 1984; *Schwartz et al.*, 1987; *Ho et al.*, 1994; *Saito et a;.*, 1996]. The changes of magnetic field and plasma density from the lobe to the central plasma sheet are found to nearly satisfy the Rankine-Hugoniot jump conditions for a slow shock.

Nevertheless, satellite observations in the Eear-earth magnetotail ($\sim$ 10-20 R_E) indicate that the structure of the near-tail plasma sheet boundary layer is very different from that in the deep tail [e.g., *Feldman et al.*, 1987; *Cattell et al.*, 1992]. The boundary layer is not usually well modeled as a time stationary slow shock. *Cattell et al.* [1992] have presented a statistical study of the MHD structure of the plasma sheet boundary layer in the near-tail, using data from the AMPTE/IRM spacecraft. They showed that the measured change in the tangential velocity across the boundary is usually much less than the velocity change predicted for a stationary slow shock. The change in plasma density appears to be much greater than that for a slow shock. In some observations near a substorm neutral line, only a portion of the boundary is consistent with being a slow shock [*Feldman et al.*, 1987]. These observations may indicate the presence of nonsteady slow shocks in a transient stage of a time-dependent magnetic reconnection.

In addition, field-aligned plasma jets are observed near the plasma sheet boundary layer [*DeCoster and Frank*, 1979; *Eastman et al.*, 1985]. An earthward plasma beam may originate from a magnetic reconnection in the magnetotail [*Sato et al.*, 1992; *Lee and Yan*, 1992], while the presence of the ionosphere on the earthward side of the X line may result in a tailward plasma beam in the plasma sheet boundary layer, leading to the complicated structure of the near-Earth reconnection [*Hesse and Birn*, 1991; *Cattell et al.*, 1992].

One-dimensional (1-D) hybrid simulations have been carried out to study the structure of the quasi-steady reconnection layer in the magnetotail [*Fujimoto and Nakamura*, 1994; *Lin and Lee*, 1995]. The simulation study by *Lin and Lee* [1995] found that in the symmetric case with exactly antiparallel magnetic field in the two lobes ($B_y = 0$), the Petschek reconnection layer with two slow shocks exists. The slow shocks are switch-off shocks, in which the intermediate Mach number $M_I = 1$ and the downstream tangential magnetic field is equal to zero, where $M_I = V_{nu}/C_{Iu}$ and V_{nu} and C_{Iu} are the normal components of flow velocity and Alfven velocity, respectively, in the upstream region. In the presence of a finite guide field ($B_y \neq 0$) in the two lobes, which has been found from the satellite observations in the magnetotail [e.g., *Fairfield*, 1979], the slow shock becomes a nonswitch-off shock with $M_I < 1$, and two rotational discontinuities are also present to bound the reconnection from the two respective lobes. In the cases with an asymmetry in plasma density and magnetic field in the lobes, an intermediate shock may also be present in the reconnection layer. Moreover, the simulation shows that a left-hand, circularly polarized wave train is present in the downstream region of switch-off slow shocks, which is consistent with the two-fluid theory of slow shocks [*Coroniti*, 1971]. The coherent wave train, however, does not exist in the non-switch-off shocks with $M_I < 0.98$, a finding consistent with the simulation study by *Lee et al.* [1989] for isolated slow shocks. *Lin and Lee* [1991] have suggested that the chaotic ion orbits may contribute to the ion heating and wave train damping in slow shocks. The dissipation in slow shocks is thus caused mainly by the chaotic ion motion. These simulation studies suggests that the lack of a coherent wave train in the slow shocks observed in the distant tail [e.g., *Feldman et al.*, 1984; *Smith et al.*, 1984] may be due to the presence of non-switch-off shocks.

The structure of collisionless slow shocks has also been studied by *Swift* [1983], *Winske et al.* [1985], *Lee et al.* [1989], *Omidi and Winske* [1989], and *Vu et al.* [1992]. Coherent wave trains have been found in the switch-off shocks [e.g., *Swift*, 1983]. On the other hand, a number of other mechanisms have also been proposed to explain the lack of coherent wave trains in the slow shocks observed in the magnetotail. *Winske and Omidi* [1990] have suggested that the electromagnetic ion/ion cyclotron instability may lead to the ion heating and damping of the downstream wave train, and *Vu et al.* [1992] have shown that the downstream boundary conditions may result in a slow shock without a wave train. In addition, *Fujimoto and Nakamura* [1994] have suggested that the damping of the coherent waves in slow shocks may be associated with the presence of heavy ions in the magnetotail.

A recent 2-D hybrid simulation by *Krauss-Varban and Omidi* [1995] has shown a large-scale outflow region in magnetic reconnection in the magnetotail. The ion kinetic physics is studied for transient plasmoids and a quasi-steady outflow region.

In order to understand the magnetic reconnection in the magnetotail it is important to study the reconnection layer by using a multi dimensional kinetic approach. In this paper we extend our 1-D hybrid simulations for the Riemann problem associated with the magnetotail reconnection layer [*Lin and Lee*, 1995] to the 2-D reconnection configuration in the distant magnetotail. We examine the structure of discontinuities in the 2-D reconnection layer and also the evolution of the discontinuities from transient stages to the steady state of a reconnection. In particular, the structure of MHD discontinuities in the quasi-steady reconnection layer is investigated. The 2-D structure of the reconnection layer is compared with our 1-D hybrid simulations.

The simulation model is given in section 2. Our simulation results are presented in sections 3 and 4. In section 3 we show the simulations for the symmetric case with $B_y = 0$ in the two lobes. The effects of a finite guide field B_y in the lobes are studied in section 4. Finally, a summary is given in section 5.

2. Simulation Model

Our 2-D hybrid simulation utilizes the hybrid code presented by *Swift* [1995, 1996], which has been used in a general curvilinear coordinate system to model the Earth's magnetosphere, while in this study we use a Cartesian coordinate system to model the magnetic reconnection in the magnetotail plasma sheet. In the hybrid code, ions are treated as discrete particles, and electrons are treated as a massless fluid. Quasi charge neutrality is assumed.

The equation for ion motion is given by

$$\frac{d\mathbf{V}_i}{dt} = \mathbf{E} + \mathbf{V}_i \times \mathbf{B} - \nu(\mathbf{u}_i - \mathbf{u}_e) \tag{1}$$

where $\mathbf{V}_i$ is the ion particle velocity, $\mathbf{E}$ is the electric field in units of ion acceleration, $\mathbf{B}$ is the magnetic field in units of the ion gyrofrequency, ν is the collision frequency which is used to model the resistivity at the X line, and $\mathbf{u}_e$ and $\mathbf{u}_i$ are the bulk flow velocities of electrons and ions, respectively. The electron momentum equation for a zero electron pressure is written in the form

$$\mathbf{E} = -\mathbf{u}_e \times \mathbf{B} - \nu(\mathbf{u}_e - \mathbf{u}_i) \tag{2}$$

The electron flow speed is evaluated from Ampere's law,

$$\mathbf{u}_e = \mathbf{u}_i - \frac{\nabla \times \mathbf{B}}{\alpha N} \tag{3}$$

where $\alpha = (4\pi e^2/m_i c^2)$, e is the electron charge, m_i is the ion mass, and N is the ion number density. In the calculation the charge coupling constant α is chosen as a scaling parameter. Note that $(N\alpha)^{-1}$ is the ion inertial length in the units used in the simulation. With the use of (2) and (3), (1) can be written as

$$\frac{d\mathbf{V}_i}{dt} = \mathbf{E}_p + \mathbf{V}_i \times \mathbf{B} \tag{4}$$

where

$$\mathbf{E}_p = (\frac{\nabla \times \mathbf{B}}{\alpha N} - \mathbf{u}_i) \times \mathbf{B} \tag{5}$$

The magnetic field is advanced in time from Faraday's law

$$\frac{\partial \mathbf{B}}{\partial t} = -\nabla \times \mathbf{E} \tag{6}$$

where the electric field is calculated from (2).

In the simulation the ion particle velocity is updated at half time step with a second-order accuracy. The magnetic field and the particle positions are advanced at the whole time step. The magnetic field update uses a predictor-corrector, or leapfrog trapezoidal, scheme. For the magnetic field time step to satisfy the Courant condition with respect to the whistler mode, the code uses a subcycling of the advance of magnetic field to the advance of particles. In our simulation the magnetic field is advanced 10 to 20 time steps for every time step the ion velocities are advanced.

In our simulation, initially at time $t = 0$, a current sheet separates the two lobes with antiparallel magnetic field component B_x in the x direction and a common guide field B_y in the y direction. The normal of the current sheet is in the z direction, and the current sheet is located along $z = 0$. The thermal plus magnetic pressure is balanced across the initial current sheet, and thus the current sheet is a tangential discontinuity. Our interest is only in the large-scale structure in the outflow region of a magnetic reconnection and not in the process that causes the reconnection to occur. A finite resistivity is imposed at the center of the simulation domain, $(x, z) = (0, 0)$, to trigger and control the reconnection. The simulation is for a spontaneous reconnection [e.g., *Scholer*, 1989], and the dynamics is non driven. The energy of the reconnection structure essentially stems from the energy of the original unperturbed states.

At the boundaries $x = \pm L_x/2$ the magnetic field is extrapolated on the basis of a zero curl and divergence of the field. The plasma flow velocity is free. At the boundaries $z = \pm L_z/2$, B_z is set to be zero for a fast magnetic reconnection, and initially there is no inflow velocity at these boundaries. We have also simulated the cases in which a small flow velocity is assumed in the inflow boundaries ($z = \pm L_z$). The results are very similar to those shown in this paper.

In the 2-D simulation, all the dependent variables are functions of the coordinate x and z and the time t. Initially, symmetric magnetic field and plasma density on the two sides of the current sheet, i.e., in the two lobes, are assumed.

In the simulation the number of ions per cell, N, in the two lobes is chosen to be $N_0 = 20$, where the subscript "0" represents the quantities in the lobes. The cell size in the z direction is chosen to be $\Delta z = 0.3\lambda_0$, where $\lambda_0 = c/\omega_{pi0}$ is the lobe ion inertial length. The cell size in the x direction is $\Delta x = 2\Delta z$. The plasma beta in the lobes is assumed to be $\beta_0 = 0.1$ in the simulation, which corresponds to an ion gyroradius $\rho_{i0} = 0.3\lambda_0$. The electron temperature is assumed to be zero. The length of the simulation domain is $L_x = 200\lambda_0$ in the x direction and $L_z = 100\lambda_0$ in the z direction. For an ion number density $N_0 \sim 0.05\text{cm}^{-3}$ in the lobe, this value corresponds to a system length of 32 R_E in the x direction. The spatial profile of the resistivity imposed in the simulation corresponds to a collision frequency

$$\nu = \nu_0 e^{-(x^2+z^2)/\lambda_0^2} \tag{7}$$

where $\nu_0 = 1.5\Omega_0$ and Ω_0 is the ion gyrofrequency in the lobes. In the simulation the time step to advance the ion velocity is chosen to be $\Delta t = 0.02\Omega_0$.

The initial profile of the x component magnetic field is given by

$$B_x(z) = B_{x0}\tanh[z/\delta] \tag{8}$$

where B_{x0} is the x component magnetic field in the

lobes and δ is the half width of the initial current sheet, which is chosen to be equal to λ_0. The profile of the y component magnetic field is assumed to be

$$B_y(z) = B_{y0} \tag{9}$$

where B_{y0} is the guide field in the lobes. The profile of ion thermal pressure is determined from the total pressure balance across the current sheet. A constant, isotropic temperature profile is assumed. The ion number density is thus given by

$$N(z) = N_0\{1+\frac{1}{\beta_0}[1-(B_{x0}^2/B_0^2)\tanh^2(z/\delta)-(B_{y0}^2/B_0^2)]\} \tag{10}$$

where $B_0 = (B_{x0}^2 + B_{y0}^2)^{1/2}$ is the total magnetic field in each lobe.

In the simulation the time is in units of Ω_0^{-1}. For the results shown in this paper the magnetic field is expressed in units of B_0, the ion number density in units of N_0, and the temperature in units of the lobe temperature T_0. The velocity is normalized to the lobe Alfven speed V_{A0}, and the spatial coordinate is normalized to λ_0.

To understand the relation between the 2-D simulation and our 1-D hybrid simulation for the Riemann problem associated with a magnetic reconnection [*Lin and Lee*, 1995], we also compare our 2-D results with the 1-D simulations. The 1-D hybrid code used in our study is that originally described by *Swift and Lee* [1983]. In the 1-D simulation a nonzero normal component of magnetic field $B_n = B_z$ is introduced into the simulation system at $t = 0$, corresponding to the occurrence of a magnetic reconnection in which B_n is present along the reconnected field lines. The initial current sheet, which has a total pressure balance, then evolves with time, and various MHD discontinuities are formed. The 1-D simulation does not include the spatial variation in the x direction. The 2-D effects on the structure of the reconnection layer are discussed in this paper.

We present simulations for two typical cases. Case 1 is a symmetric case with exactly antiparallel magnetic fields ($B_y = 0$) in the lobes, corresponding to the *Petschek* [1964] model of a fast magnetic reconnection. Since a finite B_y may be present in the tail lobes [e.g., *Fairfield*, 1979], in case 2 the presence of a nonzero guide field B_y is considered.

3. Case 1: $B_y = 0$ in the Two Lobes

In case 1 the magnetic field strengths and plasma densities are equal in the two lobes, with $B_{x1} = B_{x2} = B_{x0} = B_0$ and $N_1 = N_2 = N_0$, where the subscripts "1" and "2" represent the quantities in the north and south lobes, respectively. The guide field $B_y = 0$ on the two sides of the initial current sheet. The plasma beta $\beta_0 = 0.1$ in the two lobes.

The left column of Figure 1 shows, from the top, the configurations of magnetic field lines, ion flow velocity vectors in the xz plane, and the contour plots of ion number density N, thermal pressure P, and parallel temperature $T_\parallel$ at $t = 120\Omega_0^{-1}$. The right column of Figure 1 shows the simulation results at $t = 280\Omega_0^{-1}$. Notice that the the left column shows only the central part of the simulation domain.

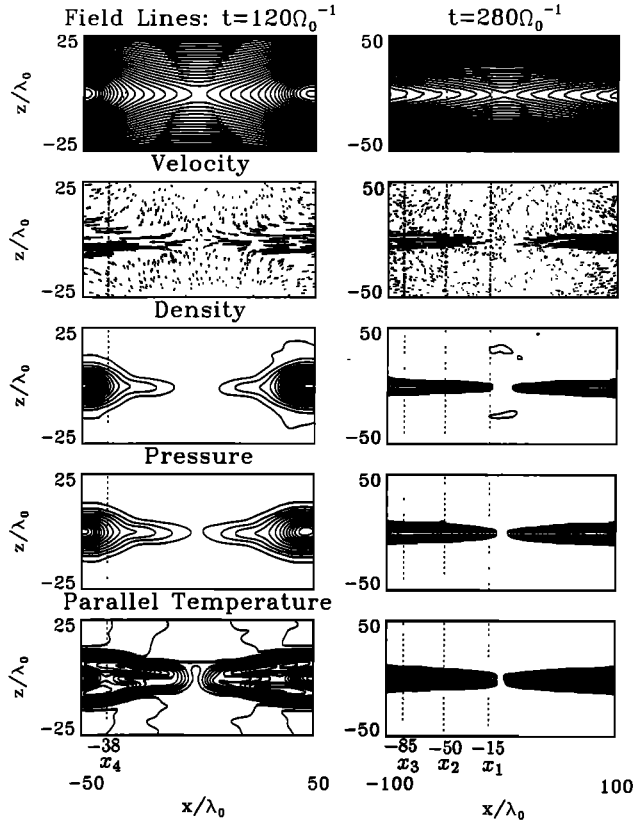

Figure 1. Configurations of magnetic field lines, velocity vectors, and contours of ion number density, thermal pressure, and parallel temperature at (left) $t = 120\Omega_0^{-1}$ and (right) $t = 280\Omega_0^{-1}$ in case 1. The four vertical dotted lines correspond to the four positions with $x = x_1 = -15\lambda_0$, $x = x_2 = -50\lambda_0$, $x = x_3 = -85\lambda_0$, and $x = x_4 = -38\lambda_0$.

An outflow region develops after the onset of a magnetic reconnection at the X line, which is located at the origin. In the outflow region the plasma is accelerated in the $z < 0$ ($z > 0$) region toward the left (right) side boundary, as shown in the streamline plots. It is seen from the field line configuration and the contour plots in Figure 1 at $t = 120\Omega_0^{-1}$ that a leading bubble-like field configuration is formed in the left as well as right part of the outflow region. A decrease in magnetic field and enhancements in plasma flow speed, density, and pressure are present in the outflow region.

On the other hand, in the region near the X line with $|x| < 20\lambda_0$, the region with the decreased magnetic field and increased ion density and pressure is much narrower than the leading bulge. Two pairs of relatively straight fronts of phase-standing shocks are formed to emanate in the xz plane from the X line. These fronts extend to the bulge regions, where they become curved, as seen from the field plot and the density and pressure contours in the left column of Figure 1. The straight shock

fronts are associated with a quasi-steady reconnection layer. This region with steady shock fronts elongates with the duration of the magnetic merging event. Our analysis indicates that the shocks are slow shocks, a finding discussed later in this paper.

At a later time with $t = 280\Omega_0^{-1}$, which nearly corresponds to 7 min for a lobe field $B_0 \sim 7$ nT, the bulge region of magnetic field has moved out of the simulation domain, and only the steady reconnection layer appears, as shown in the right column of Figure 1. The angle between each shock front and the x axis is found to be $\gamma = 3.8^o$. The plasma is accelerated by the slow shocks from upstream (lobe) to downstream (plasma sheet), while the slow shocks are located in the plasma sheet boundary layer region in the magnetotail. It is found that the magnetic field in the upstream region of each shock is slightly smaller than the initial lobe field, as a result of the presence of a fast mode expansion wave upstream of the shock [*Lin and Lee*, 1994]. This fast wave quickly propagates away from the reconnection layer. It leads to the presence of a finite plasma inflow velocity upstream of the slow shock, which has a component in the $-z$ direction.

In general, at the transient stage of a reconnection a leading bulge-like magnetic configuration and a trailing reconnection layer are usually formed [see also *Scholer*, 1989; *Shi and Lee*, 1990; *Semenov et al.*, 1992; *LaBelle-Hamer et al.*, 1994]. If the duration of reconnection is short, the bulge-like structure will dominate the plasma outflow region. If magnetic reconnection occurs over a long time, the trailing reconnection layer will dominate.

Figure 2 shows the ion velocity distributions at locations in the $z > 0$ region along $x = x_3 = -85\lambda_0$ at $t = 280\Omega_0^{-1}$ and $x = x_4 = -38\lambda_0$ at $t = 120\Omega_0^{-1}$, where x_3 is located in the trailing reconnection layer region and x_4 is in the leading bulge region, as shown by the dashed lines in Figure 1. The left, middle, and right plots of the top panel of Figure 2 show the distributions of ion velocities in the xz plane at the positions s_1 with $z = 7.5\lambda_0$, s_2 with $z = 4.5\lambda_0$, and s_3 with $z = 0.3\lambda_0$, respectively, along $x = x_3$. The solid line in each plot is aligned with the corresponding magnetic field direction. Note that the position s_1 is just at the upstream edge of the slow shock, s_2 is in the shock transition region, and s_3 is nearly at the plasma sheet center downstream of the slow shock. At s_1 a relatively cold plasma has a small flow velocity along the $-z$ direction. At s_2, two parts of ions are seen in the velocity contour plot at s_2. One is the ions accelerated by the slow shock, which has an earthward ($x < 0$) bulk flow speed nearly equal to the upstream Alfven speed, and the other is associated with the low-speed lobe ions. While the two streams of ions mix, the parallel ion temperature is enhanced in the plasma sheet boundary layer. At position s_3, only the ions which are heated by the slow shock is seen. In addition, some downstream ions also stream back to the upstream of the shock, as shown in the left plot of Figure 2. A strong temperature anisotropy with $T_\parallel > T_\perp$ is found in the transition region of the slow shock, as will be shown later in this section, where $T_\parallel$ and $T_\perp$ are the temperatures parallel and perpendicular to the magnetic field, respectively. The backstreaming ion beam has also been found in the 1-D hybrid simulations of the reconnection layer [*Fujimoto and Nakamura*, 1994; *Lin and Lee*, 1995], 2-D hybrid simulations of magnetic reconnection [e.g., *Krauss-Varban and Omidi*, 1995], and satellite observations in the magnetotail [e.g., *Saito et al.*, 1996]. Because the ionosphere is not considered in our simulation, no tailward beam is observed in the plasma sheet boundary layer. In the upstream region, e.g., at point S_1, $T_\perp$ is much larger than $T_\parallel$, consistent with the recent GEOTAIL observation reported by *Saito et al.* [1996].

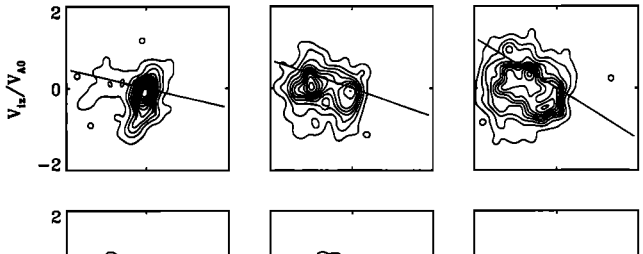

Figure 2. (Top) Ion velocity distributions (left) upstream, (middle) in the transition region, and (right) downstream of the slow shock in case 1 along $x = x_3$. The quantities V_{ix} and V_{iz} indicate the ion velocities in the x and z directions, respectively. (Bottom) Velocity distribution (left) in the lobe, (middle) in the plasma sheet boundary layer, and (right) in the plasma sheet center along $x = x_4$. The solid line in each plot is aligned with the corresponding magnetic field direction.

The ion velocity distributions along $x = x_4$ are shown in the bottom panel of Figure 2. The left, middle, and right plots correspond to the positions at s_4 with $z = 7.5\lambda_0$, s_5 with $z = 3.6\lambda_0$, and s_6 with $z = 0.3\lambda_0$, respectively. At position s_4 the bulk flow velocity of ions is nearly zero. In the plasma sheet boundary layer, two parts of ions with different flow velocities exist, as shown in the middle plot for s_5. Near the plasma sheet center at position s_6 the ion velocity distribution is more isotropic. The above result at the transient stage of the magnetic reconnection is very similar to that in the quasi-steady reconnection layer.

The shocks are formed from the disturbances at the site of reconnection, i.e., at the X line. A clear separation between the two slow shocks in case 1 requires a sufficient distance from the X line along the x axis. Near the X line the shocks may be too close to each other, and the downstream region of each shock is not well developed, so that the change of physical quantities across each shock does not satisfy the Rankine-Hugoniot jump conditions for a steady slow shock. At a larger distance from the X line it is expected that the agreement with the Rankine-Hugoniot conditions is improved.

The left three columns of Figure 3 show the profiles of B_x, B_y, B_z, magnetic field strength B, ion flow velocity components V_x, V_y, and V_z, ion number density N, $T_\parallel$, and $T_\perp$ at $t = 280\Omega_0^{-1}$ as a function of z at $x = x_1 = -15\lambda_0$, $x = x_2 = -50\lambda_0$, and $x = x_3 = -85\lambda_0$. The three positions x_1, x_2, and x_3 are indicated in the right column of Figure 1, corresponding to the three different distances from the X line in a quasi-steady reconnection. At each of the three positions, two shock fronts are present, whose positions are indicated by the two dashed lines at a and b. in Figure 3. Across each front from upstream to downstream the magnetic field decreases, while the ion number density, flow speed, and temperature increase. Among the three positions $x = x_1$, x_2, and x_3, x_1 is the nearest to the X line, and the two shock fronts are the closest to each other. The increase of plasma flow speed across the slow shock at $x = x_1$ is only about 0.4 of the upstream Alfven speed V_{A0}, and the increases in ion number density and temperature are also small, as shown in the left column of Figure 3. At $x = x_2$ the two shocks are more separated from each other, and the increases of flow velocity, plasma density, and temperature at the slow shock become larger. At $x = x_3$, the point farthest away from the X line, the separation distance between the two slow shocks is the largest. Correspondingly, the largest enhancement in flow velocity among the three positions is obtained, which is very close to the upstream Alfven speed.

The jumps of magnetic field and plasma quantities across the shock on the $z > 0$ side at $x = x_3$ are estimated as follows. For the shock front, which has an angle γ relative to the x axis, the tangential component of the magnetic field at the shock is given by

$$B_t = B_x\cos\gamma - B_z\sin\gamma \tag{11}$$

and the normal component is given by

$$B_n = |B_z\cos\gamma + B_x\sin\gamma| \tag{12}$$

In the upstream region the magnetic field components are found to be $B_{xu} \simeq 0.91B_0$, $B_{yu} \simeq 0$, and $B_{zu} \simeq -0.18B_0$. For $\gamma = 3.8^o$ the tangential and normal components of the upstream magnetic field are thus $B_{tu} \simeq 0.92B_0$ and $B_{nu} = 0.12B_0$, respectively. The shock normal angle $\theta_{nB} = \tan^{-1}(B_{tu}/B_{nu}) \simeq 82.5^o$. In the downstream region of the shock, which is at the center with $z \simeq 0$, the magnetic field components are found to be $B_{xd} \simeq 0$, $B_{td} \simeq 0.007B_0$, and $B_{nd} \simeq 0.12B_0$. Note that $B_{nu} \simeq B_{nd} = B_n$, consistent with the Rankine-Hugoniot conditions of a steady shock. The ratio of downstream to upstream tangential magnetic field is thus $R_{Bt} \simeq 0.01$. The normal component of the flow velocity is found to be $V_{nu} \simeq 0.17V_{A0}$ upstream and $V_{nd} \simeq 0.055V_{A0}$ downstream. Therefore we have $V_{nd}/V_{nu} \simeq 0.32$. The ratio of downstream to upstream ion number density is found to be $R_N = N_d/N_u \simeq 3.2$. Thus we have $N_d/N_u \simeq V_{nu}/V_{nd}$, as expected for a quasi-steady shock. Upstream of the shock front the plasma beta is found to be $\beta_u \simeq 0.1$. The intermediate Mach number of the shock is $M_I = V_{nu}/C_I \simeq 0.85$, where $C_I = C_{I0}(1-\alpha_u)^{1/2} \simeq 0.20$ is the upstream in-

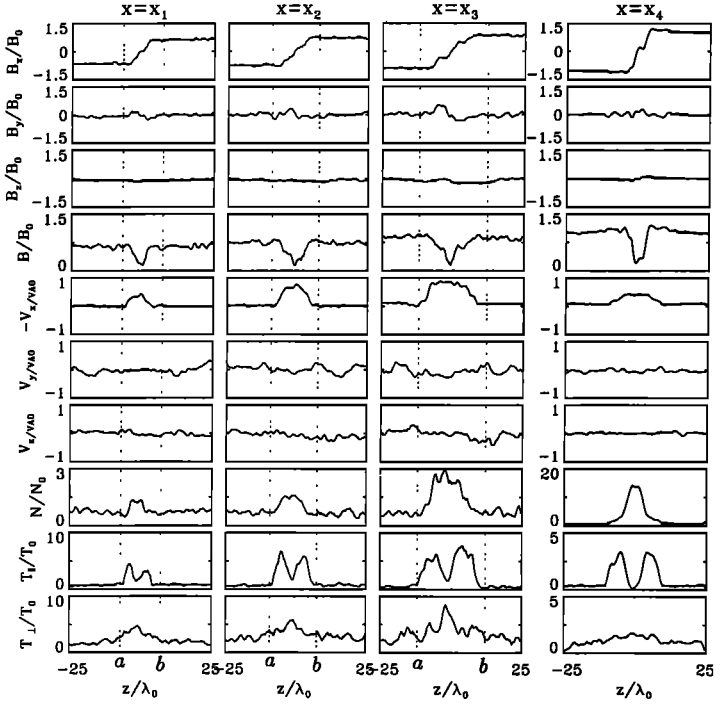

Figure 3. Spatial profiles of B_x, B_y, B_z, magnetic field strength B, velocity components V_x, V_y, and V_z, ion number density N, and the temperatures $T_\parallel$ and $T_\perp$ along $x = x_1$, x_2, x_3, and x_4 in case 1. The vertical dotted lines at positions a and b indicate the fronts of two slow shocks.

termediate mode speed in a plasma with a temperature anisotropy, C_{I0} is the MHD intermediate mode speed, and $\alpha_u = (\beta_{\|} - \beta_{\perp})/2$ measures the degree of temperature anisotropy. Note that in this case α_u is found to be approximately -0.06, and α_d in the downstream region is approximately -17. On the other hand, the ratios of magnetic field and plasma density obtained from the Rankine-Hugoniot jump conditions for the slow shock [*Chao*, 1970] with $\beta_0 = 0.1$, $\theta_{nB} = 82.5°$, $M_I = 0.85$, $\alpha_u = -0.06$, and $\alpha_d = -17$ are $R_{Bt} = 0.026$ and $R_N = 3.1$, respectively. Therefore the jumps in magnetic field, ion density, and normal flow velocity estimated from our simulation are found to be close to those from the Rankine-Hugoniot jump conditions for the slow shock.

Nevertheless, the velocity change $(V_{td} - V_{tu})$ across the slow shock is found to be $0.83V_{A0}$, which is still considerably less than the predicted value $1.3V_{A0}$, from the jump conditions. Note that the predicted velocity change across the slow shock is greater than the initial upstream Alfven speed V_{A0} because of the temperature anisotropy developed in the reconnection layer. In addition, the measured temperature ratios are $R_{T_{\|}} = T_{\|d}/T_{\|u} \simeq 5.0$ and $R_{T_{\perp}} = T_{\perp d}/T_{\perp u} \simeq 3.0$, while the Rankine-Hugoniot jump conditions predict $R_{T_{\|}} = 6.0$ and $R_{T_{\perp}} = 3.8$. Notice that the magnetic field decreases slowly and reaches zero only at $z \sim 0$, an indication that transition layer of the shock has not fully developed. This may cause the Rankine-Hugoniot jump conditions not to be perfectly satisfied at the shock. It is expected that the full development of the slow shocks can be obtained at a distance from the X line where the separation between the shocks is greater than a few tens of λ_0.

The slow shock in the $z < 0$ region at $x = x_3$ is also found to nearly satisfy the Rankine-Hugoniot jump conditions. At $x = x_1$ and x_2, however, the Rankine-Hugoniot jump condition for the slow shock are less satisfied.

Note that the slow shocks in the 2-D simulation of case 1 are not switch-off shocks, while in the 1-D simulation two switch-off shocks are present in the symmetric case with $B_y = 0$ in the two lobes. Because of the finite angle between the shock front and the x axis the magnetic field with $B_{xd} = 0$ does not mean $B_{td} = 0$.

On the other hand, the right column of Figure 3 shows the spatial profiles of various quantities at $x = x_4 = -38\lambda_0$ at $t = 120\Omega_0^{-1}$, which is located in the bulge region of the magnetic field. The magnetic field decreases and ion number density and flow speed increase from either lobe region to the plasma sheet center ($z \sim 0$). This structure looks like a slow shock. The profiles, however, appear to be very different from those in the steady reconnection layer region at $x = x_1$, x_2, and x_3. The increase in ion number density is much larger than that expected from the Rankine-Hugoniot jump conditions of a steady slow shock, e.g., at $x = x_3$. Meanwhile, the acceleration of plasma flow is much less than that at the steady shock, as seen from the velocity profiles. The curved front in the bulge region in Figure 1 cannot be identified as a steady shock. This structure is evolving with time as the bulge region propagates. The shock normal angle of this time-dependent structure is smaller than that of the steady part in the trailing reconnection layer.

For comparison, Figure 4 shows our 1-D hybrid simulation results for case 1. The left, middle, and right panels show spatial profiles of B_x, V_x, and N, respectively, for a time sequence from $t = 0$ to $t = 425\Omega_0^{-1}$. Note that the x component is tangential to the normal direction in the 1-D simulation. Two slow switch-off shocks develop in the reconnection layer. The intermediate Mach number of the switch-off shock is $M_I \simeq 1$. The shock front of the slow shock on the $z < 0$ ($z > 0$) side propagates to the lobe in the $+\mathbf{z}$ ($-\mathbf{z}$) direction along pp' (qq'), as shown in Figure 4. The ion number density, flow speed, and temperature increase across each slow shock. In the downstream region the magnetic field possesses a large-amplitude, left-hand-polarized helical wave train. The downstream magnetic field oscillates around the tangential field $B_t = 0$, as seen from the B_x profile. A consistent wave structure is also seen in the

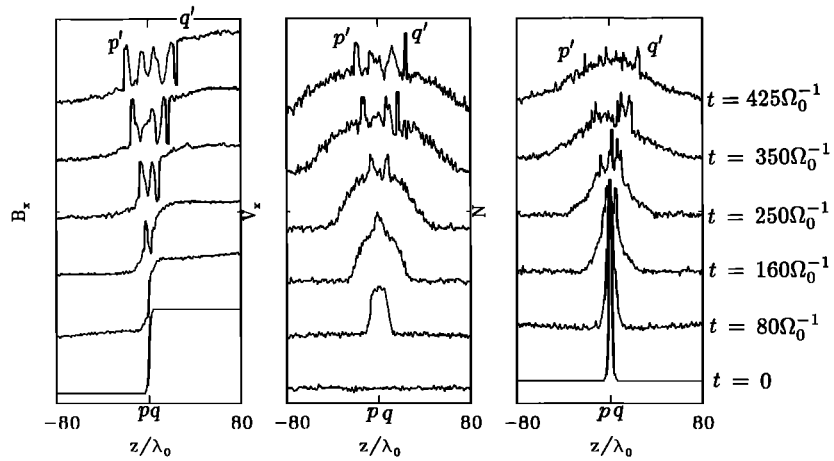

Figure 4. Spatial profiles of B_x, V_x, and N in a time sequence obtained from the 1-D simulation of case 1. The fronts of two slow shocks propagate along pp' and qq'.

ion flow velocity profile. Similarly to the 2-D simulation result, a significant increase in $T_{\parallel}$ is found in the shock layer, and a backstreaming ion beam is present in the upstream region of the slow shocks. Note that in the 1-D simulation the decrease of ion number density from the initial value at the center of the current sheet is much slower than that in the 2-D simulation. The two shock fronts propagate away from each other with time. The clear downstream structure can be seen only when the two shocks are separated by a sufficient distance, which corresponds to a long enough simulation time.

The time t in the 1-D simulation corresponds roughly to the distance x from the X line in the 2-D steady reconnection configuration [*Lin and Lee*, 1994, 1995]. At a distance x near (far from) the X line the profiles of physical quantities along z are similar to the profiles in the 1-D simulation at an early (late) time.

The large-amplitude rotational wave train in the magnetic field, present in the 1-D simulation of case 1, is not seen in the 2-D simulation shown in Figure 1. *Lee et al.* [1989] and *Lin and Lee* [1995] have suggested that the lack of a coherent wave train in slow shocks may be due to the fact that the slow shock is a non-switch-off shock. In 1-D simulations of the reconnection layer the slow shocks become non-switch-off shocks if the guide field B_{y0} is nonzero in the lobes. The coherent wave train is found to disappear when $B_{y0} > 0.08B_{x0}$, which corresponds to a non-switch-off shock with $M_I < 0.98$ for $\theta_{nB} = 75^o$. In the above 2-D hybrid simulation, the slow shocks are non-switch-off shocks because the shock front angle $\gamma \neq 0$. This inequality may lead to the disappearance of the coherent wave train. In addition, it is also likely that the separation between the two slow shocks in Figure 1 is not large enough for the downstream structure to become fully developed.

The appearance of slow shocks has also been found from 2-D MHD theories [e.g., *Semenov et al.*, 1992] and simulations [e.g., *Sato*, 1979; *Shi and Lee*, 1990; *Yan et al.*, 1992] for the *Petschek* [1964] type reconnection. The decrease in magnetic field and increase in plasma density and temperature across the slow shock have been obtained. Nevertheless, the kinetic structure of slow shocks in a collisionless plasma cannot be studies by the MHD models.

The simulation of case 1 suggests that the lack of a coherent wave train in slow shocks observed in the distant magnetotail may be due to the 2-D effects of the reconnection layer, which lead to the presence of non-switch-off shocks, as described above. The 2-D effects have also been suggested by *Lee et al.* [1989] based on 2-D MHD simulations of magnetic reconnection, which suggest that the slow shocks in most regions of the distant tail are non-switch-off shocks.

4. Cases with $B_y \neq 0$

In case 2 the x component magnetic field in the two lobes is $B_{x0} = 0.87B_0$, and the guide field $B_{y0} = 0.5B_{x0}$. The plasma density and pressure are symmetric across the initial current sheet. Note that in order to see the effects of B_y more clearly, a relatively large B_{y0} is chosen in this case. We first show the 1-D hybrid simulation of case 2. The 2-D simulation results then follow.

The left column of Figure 5 shows the hodograms of tangential magnetic field obtained from the 1-D simulation at $t = 0$, $43\Omega_0^{-1}$, $86\Omega_0^{-1}$, $129\Omega_0^{-1}$, $172\Omega_0^{-1}$, and $470\Omega_0^{-1}$. The spatial profiles of B_x (solid lines) and B_y (dotted lines) at the corresponding time instants are shown in the second column of Figure 5. The third and fourth column present the spatial profiles of V_x and N, respectively. Two discontinuities are formed in the reconnection layer. A rotational discontinuity RD1 propagates to the lobe in the $z < 0$ region. Another rotational discontinuity RD2 propagates to the lobe on the $z > 0$ side, as indicated in the top panel in Figure 5. In early times ($t < 129\Omega_0^{-1}$) the two rotational discontinuities are not separated. The B_y component only slightly increases from the lobe to the plasma sheet, while the ion number density increases greatly. The rotation of the magnetic field in the xy plane is not clear. At $t < 86\Omega_0^{-1}$ the field hodogram is almost flat, as shown in Figure 5.

On the other hand, at $t = 470\Omega_0^{-1}$, RD1 and RD2 are clearly separated. The magnetic field rotates from $B_x = -0.75B_0$ and $B_y = 0.35B_0$ to $B_x \simeq 0$ and $B_y \simeq 0.7B_0$ across the rotational discontinuity RD1. Notice that the magnetic field strength slightly decreases and ion number density increases across the rotational discontinuity. The changes in the magnetic field and ion density at the rotational discontinuity are due to the presence of $T_{\parallel} > P_{\perp}$ in most regions of the reconnection layer. The ion flow is accelerated across the rotational discontinuity and slow shock. The change of the flow velocity across the rotational discontinuity is found to be nearly equal to the change of the Alfven velocity across the discontinuity.

Our MHD simulations of case 2 indicate that there exist two slow shocks between the rotational discontinuities RD1 and RD2 [*Lin and Lee*, 1995]. The slow shocks, however, are too weak to be identified in the hybrid simulation because of the temperature anisotropy.

The 2-D hybrid simulation results of case 2 are shown in Figures 6 and 7. Figure 6 shows the configuration of magnetic field lines, the streamlines, and the contour plots of ion number density, thermal pressure, and parallel temperature in the xz plane at $t = 175\Omega_0^{-1}$ obtained from the 2-D simulation of case 2. Similarly to case 1, a leading bulge region and a trailing quasi-steady reconnection layer are formed in the outflow region of the magnetic reconnection, as shown in the magnetic field and plasma plots in Figure 6. The magnetic field decreases and plasma pressure and temperature increase across the plasma sheet boundary layer. In additon, an accelerated flow is present in the plasma sheet. Similarly to case 1, a strong enhancement in the parallel temperature is present in the plasma sheet boundary layer.

We show the profiles of various quantities along the z direction at three different x positions. Figure 7 shows the profiles at s_1 with $x = x_1 = -40\lambda_0$, s_2 with

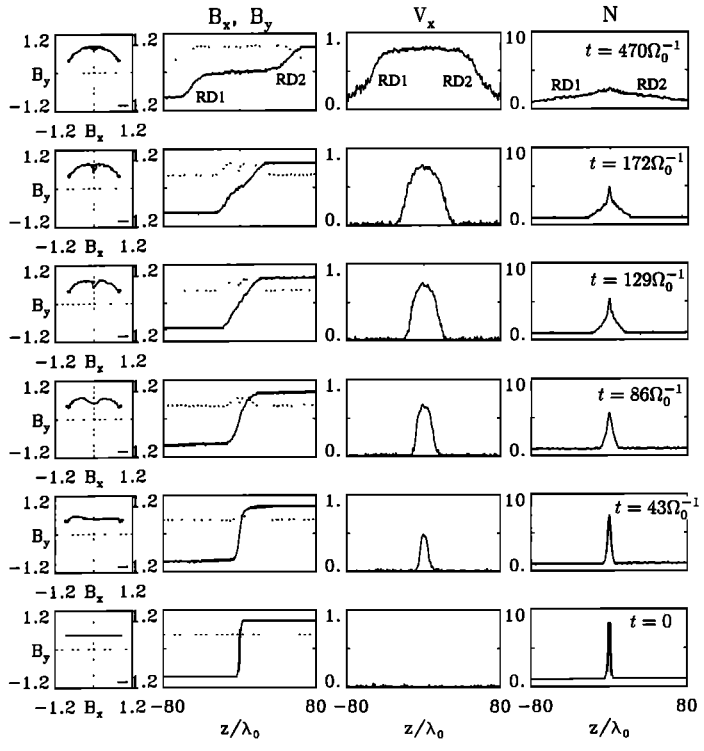

Figure 5. Hodograms of the tangential magnetic field and spatial profiles of B_x (solid line), B_y (dotted line), V_x, and N obtained from the 1-D simulation of case 2. The five panels correspond to five different times. The physical quantities are normalized to those in the lobes. The labels RD1 and RD2 indicate the two rotational discontinuities.

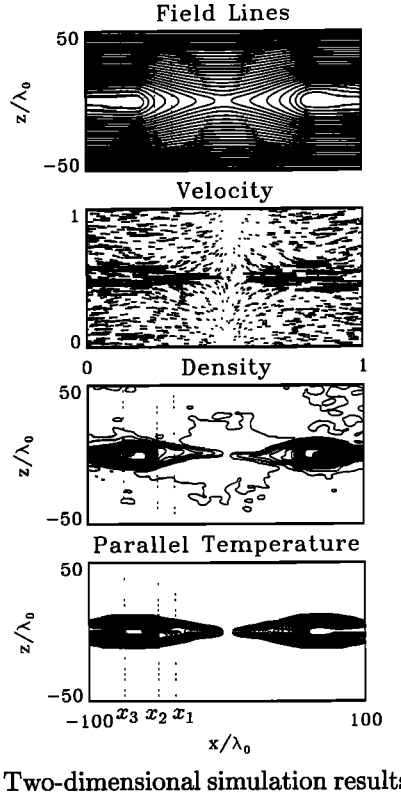

Figure 6. Two-dimensional simulation results of case 2 at $t = 175\Omega_0^{-1}$: field line configuration, flow vector plot, and the contours of ion number density and parallel temperature. The three vertical dotted lines correspond to the three positions with $x = x_1 = -40\lambda_0$, $x = x_2 = -50\lambda_0$, and $x = x_3 = -75\lambda_0$.

$x = x_2 = -50\lambda_0$, and s_3 with $x = x_3 = -75\lambda_0$. Among them, x_1 is located in the steady reconnection layer region, and x_2 and x_3 are in the leading bulge region, as indicated in Figure 7. At $x = x_1$ the B_y component of magnetic field increases across the plasma sheet boundary layer, while B_x decreases. It is found that the hodogram of tangential magnetic field at $x = x_1$ is very similar to that obtained from the 1-D simulation results at very early times. The layer that contains discontinuities appears to be gradually wider as the distance x is gradually farther away from the X line. In addition, the flow speed and ion number density increase across the boundary layer. We have run the case until the leading bulge region has moved out of the simulation domain and found that the spatial profile of the tangential magnetic field near the edge of the simulation domain is very similar to that at $x = x_1$, except the change of B_y across the boundary layer is larger.

At $x = x_2$, the B_y component of the magnetic field and plasma density are also found to increase across the boundary layer. The density increase, however, is much larger than that at $x = x_1$, as seen in Figure 7. At $x = x_3$, which is further into the leading bulge region in the 2-D reconnection configuration, an accelerated ion flow is present on either side of the plasma sheet center, indicating that the high-speed flow is also bulge-like. At the center of the plasma sheet, however, the flow speed is not large. Similarly to case 1, the bulge region evolves with time. No steady rotational discontinuity is found in this region, although the tangential magnetic field shows a rotation.

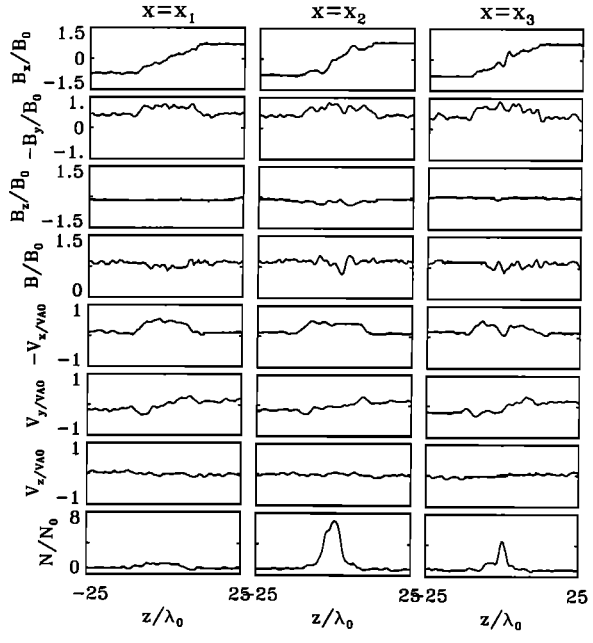

Figure 7. Spatial profiles of magnetic field, velocity, and ion number density along $x = x_1$, x_2, and x_3 in case 2.

We have also run the cases with $B_{y0} = 0.1B_0$, $0.7B_0$, and $1.0B_0$. The results are similar to those of case 2. Our 1-D hybrid simulations show that a coherent wave train exists in the reconnection layer if $B_{y0} < 0.08B_{x0}$, and the wave train disappears for the cases with $B_{y0} \geq 0.08B_{x0}$. The disappearance of the wave train is associated with the presence of non-switch-off slow shocks in the reconnection layer. In our 2-D simulation, no large-amplitude wave train structure appears in the simulation domain for the cases with $B_{y0} \neq 0$, possibly because the simulation domain is not large enough, so that the slow shocks are not well developed. In addition, the finite angle between the shock, or discontinuity, fronts and the x axis may also reduce the critical B_y above which the coherent wave does not exist.

5. Summary

We have carried out 2-D hybrid simulations to study the structure of the reconnection layer in the distant magnetotail. The results are also compared with the 1-D hybrid simulations for the corresponding cases. A summary of the simulation results are given below.

1. In general, a leading bulge-like magnetic configuration and a trailing reconnection layer are usually formed in a magnetic reconnection. If the duration of the reconnection is short, the bulge-like structure will dominate the plasma outflow region. If magnetic reconnection occurs for a long time, the steady, trailing reconnection layer will dominate.

2. For the symmetric lobes with $B_y = 0$, two pairs of slow shocks are present in the quasi-steady reconnection layer. The shock fronts emanate from the X line nearly along the x direction, with a small flaring angle toward the z direction. The full development of the slow shock structure requires a sufficient distance from the X line along the x axis, where the two shock fronts separate by more than a few tens of the lobe ion inertial lengths. It is found in our 2-D hybrid simulation that the Rankine-Hugoniot jump conditions of the slow shock become better satisfied as the x distance from the X line increases.

3. For the cases with $B_y \neq 0$ in the two lobes, two rotational discontinuity-like structures appear to develop in the quasi-steady reconnection layer. Across the structure B_y increases from the lobe to the plasma sheet.

4. In the leading bulge region of a magnetic reconnection the magnetic field configuration is time dependent. No steady MHD discontinuities are found. Across the plasma sheet boundary layer the increase of the flow velocity appears to be much smaller than that predicted from the Rankine-Hugoniot jump conditions for a steady discontinuity, and the increase in the ion number density is much larger.

5. A significant increase in the parallel ion temperature is found in the plasma sheet boundary layer. Ion velocity distributions in the boundary layer show the presence of two ion beams; one is associated with the accelerated ions by the slow shock, and the other contains the cold ion population from the lobe. In addition, a backstreaming ion beam from the downstream region is present in the upstream of the slow shock, which is seen in both the 1-D and 2-D hybrid simulations for the reconnection layer. Upstream of the slow shock, the perpendicular temperature is larger than the parallel temperature. The ion dynamics and the kinetic structure of the reconnection layer cannot be obtained from MHD simulations.

6. The 1-D simulation for the structure of the reconnection layer can be related to the 2-D steady state reconnection configuration. The time t in the 1-D simulation roughly corresponds to the distance x from the X line. The profiles of physical quantities in the 1-D simulation at an early (late) time correspond to the profiles in the 2-D simulation at a small (large) x distance from the X line. Nevertheless, because of the 2-D effects the shock structure in the 2-D simulation may be different from that in the 1-D simulation. The slow shocks in the 2-D reconnection layer with lobe $B_y = 0$ are nonswitch-off shocks, while in the 1-D simulation they are switch-off shocks with an intermediate Mach number $M_I \simeq 1$. A large-amplitude rotational wave train is present downstream of the switch-off shocks in the 1-D simulation.

7. The large-amplitude rotational wave train is not found in the present 2-D simulations for the reconnection in the magnetotail. This may result from the presence of the slow nonswitch-off shocks due to the 2-D effects. In addition, the simulation domain is not long enough for the structure of slow shocks to fully develop. Note that the coherent wave train structure of slow shocks has not been observed in the magnetotail.

In addition, other mechanisms have also been proposed to explain the lack of coherent waves in slow shocks in the magnetotail. *Lin and Lee* [1995] have shown that the presence of a finite B_y or an unequal

plasma density in the two lobes may lead to the presence of non-switch-off slow shocks and thus the disappearance of the wave train. *Winske and Omidi* [1990] have suggested that the damping of the downstream wave train in slow shocks may be associated with the electromagnetic ion/ion cyclotron instability due to the ion beams. *Fujimoto and Nakamura* [1994] have suggested that the existence of heavy ions in the magnetotail may lead to the damping of the coherent waves in slow shocks.

Our simulation indicates that a steady slow shock cannot be found in the transient stage of a magnetic reconnection in the magnetotail. In the near-tail plasma sheet boundary layer the increase of the ion density is often observed to be much higher than that for a steady shock, and the flow acceleration is much smaller [e.g., *Cattell et al.*, 1992], consistent with our simulation results in the leading bulge region of the magnetic reconnection. While the near-Earth reconnection configuration is more complicated because of the presence of the ionosphere, a further investigation with a more adequate boundary condition is needed.

Acknowledgments. This work was supported by NSF grant ATM-9507993 and ONR grant NAVY-N00014-951-0839 to the Auburn University and AFOSR grant F49620-94-0218 to the University of Alaska. Computer resources were provided by the Arctic Region Supercomputer Center and the San Diego Supercomputer Center.

The Editor thanks K. Schindler and another referee for their assistance in evaluating this paper.

References

Cattell, C. A., C. W. Carlson, W. Baumjohann, and H. Luhr, The MHD structure of the plasma sheet boundary, 1, Tangential momentum balance and consistency with slow mode shocks, *Geophys. Res. Lett., 19*, 2083, 1992.

Chao, J. K., Interplanetary collisonless shock waves, *Rep. CSR TR-70-3*, Mass. Inst. of Technol. Cent. for Space Res., Cambridge, Mass., 1970.

Coroniti, F. V., Laminar wave-train structure of collisionless magnetic slow shocks, *Nucl. Fusion, 11*, 261, 1971.

DeCoster, R. J., and L. A. Frank, Observations pertaining to the dynamics of the plasma sheet, *J. Geophys. Res., 84*, 5099, 1979.

Dungey, J. W., Interplanetary magnetic field and the auroral zones, *Phys. Rev. Lett., 6*, 47, 1961.

Eastman, T., E., L. A. Frank, and C. Y. Huang, The boundary layers as the primary transport regions of the Earth's magnetotail, *J. Geophys. Res., 90*, 1985.

Fairfield, D. H., On the average configuration of the geomagnetic tail, *J. Geophys. Res., 84*, 1950, 1979.

Feldman, W. C., et al., Evidence for slow-mode shock in the deep geomagnetic tail, *Geophys. Res. Lett., 11*, 599, 1984.

Feldman, W. C., D. N. Bakes, S. J. Bame, J. Birn, J. T. Gosling, E. W. Hones Jr., and S. J. Schwartz, Slow-mode shocks: A semipermanent feature of the distant geomagnetic tail, *J. Geophys. Res., 90*, 233, 1985.

Feldman, W. C., R. L. Tokas, J. Birn, E. W. Hones Jr., S. J. Bame, and C. T. Russell, Structure of a slow mode shock observed in the plasma sheet boundary layer, *J. Geophys. Res., 92*, 83, 1987.

Fujimoto, M., and M. Nakamura, Acceleration of heavy ions in the magnetotail reconnection layer, *Geophys. Res. Lett., 21*, 2955, 1994.

Hesse, M., and J. Birn, Plasmoid evolution in an extended magnetotail, *J. Geophys. Res., 96*, 5683, 1991.

Heyn, M. F., H. K. Biernat, R. P. Rijnbeek, and V. S. Semenov, The structure of reconnection layer, *J. Plasma Phys., 40*, 235, 1988.

Ho, C. M., B. T. Tsurutani, E. J. Smith, and W. C. Feldman, A detailed examination of an X-line region in the distant tail: ISEE-3 observations of jet flow and B_z reversals and a pair of slow shocks, *Geophys. Res. Lett., 21*, 3031, 1994.

Hones, E. W., Jr., Transient phenomena in the magnetotail and their relation to substorms, *Space Sci. Rev., 23*, 393, 1979.

Krauss-Varban, D., and N. Omidi, Large-scale hybrid simulations of the magnetotail during reconnection, *Geophys. Res. Lett., 22*, 3271, 1995.

LaBelle-Hamer, A. L., A. Otto, and L. C. Lee, Magnetic reconnection in the presence of sheared plasma flow: Intermediate shock formation, *Phys. Plasmas, 1*, 706, 1994.

Lee, L. C., and M. Yan, Structure of field-aligned plasma jets associated with magnetic reconnection, *Phys. Fluids, B4*, 3808, 1992.

Lee, L. C., Y. Lin, Y. Shi, and B. T. Tsurutani, Slow shock characteristics as a function of distance from the X-line in the magnetotail, *Geophys. Res. Lett., 16*, 903, 1989.

Levy, R. H., H. E. Petschek, and G. L. Siscoe, Aerodynamic aspects of the magnetospheric flow, *AIAA J., 2*, 2065, 1964.

Lin, Y., and L. C. Lee, Chaos and ion heating in a slow shock, *Geophys. Res. Lett., 18*, 1615, 1991.

Lin, Y., and L. C. Lee, Structure of reconnection layers in the magnetosphere, *Space Sci. Rev., 65*, 59, 1994.

Lin, Y., and L. C. Lee, A simulation study of the Riemann problem associated with the magnetotail reconnection, *J. Geophys. Res., 100*, 19,227, 1995.

Omidi, N., and D. Winske, Structure of slow magnetosonic shocks in low beta plasmas, *Geophys. Res. Lett, 16*, 907, 1989.

Petschek, H. E., Magnetic field annihilation, in AAS-NASA Symposium on the Physics of Solar Flares, *NASA Spec. Publ., SP-50*, 425-439, 1964.

Russell, C. T., and R. C. Elphic, Initial ISEE magnetometer results: Magnetopause observations, *Space Sci. Rev., 22*, 691, 1978.

Saito, Y., T. Mukai, T. Terasawa, A. Nishida, S. Machida, S. Kokubun, and T. Yamamoto, Foreshock structure of the slow-mode shocks in the Earth's magnetotail, *J. Geophys. Res., 101*, 13,267, 1996.

Sato, T., Strong plasma acceleration by slow shocks resulting from magnetic reconnection, *J. Geophys. Res., 84*, 7177, 1979.

Sato, T., T. Hayashi, K. Watanabe, R. Horiuchi, and M. Tanaka, Role of compressibility on driven magnetic reconnection, *Phys. Fluids., B4*, 450, 1992.

Scholer, M., Undriven magnetic reconnection in an isolated current sheet, *J. Geophys. Res., 94*, 8805, 1989.

Scholer, M., and D. Roth, Simulation study on reconnection and small-scale plasmoid formation, *J. Geophys. Res., 92*, 3223, 1987.

Schwartz, S. J., M. F. Thomsen, W. C. Feldman, and F. T. Douglas, Electron dynamics and potential jump across slow mode shocks, *J. Geophys. Res., 92*, 3165, 1987.

Semenov, V. S., I. V. Kubyshkin, V. V. Lebedera, M. V. Sidneva, R. P. Rijnbeek, M. F. Heyn, H. K. Biernat, and C. J. Farrugia, A comparison and review of steady-state reconnection and time-varying reconnection, *Planet. Space Sci., 40*, 63, 1992.

Shi, Y., and L. C. Lee, Structure of the reconnection layer at the dayside magnetopause, *Planet. Space. Sci., 38*, 437, 1990.

Smith, E. J., J. A. Slavin, B. T. Tsurutani, W. C. Feldman,

and S. J. Bame, Slow mode shocks in the Earth's magnetotail: ISEE-3, *Geophys. Res. Lett., 11*, 1054, 1984.

Sonnerup, B. U. O., Magnetic field reconnection, in *Solar System Plasma Physics, vol. III*, edited by C. F. Kennel, L. T. Lanzerotti, and E. N. Parker, p.45, North Holland, New York, 1979.

Sonnerup, B. U. O., G. Paschmann, I. Papamastorakis, N. Sckopke, G. Haerendel, S. J. Bame, J. R. Asbridge, J. T. Gosling, and C. T. Russell, Evidence for magnetic reconnection at the Earth's magnetopause, *J. Geophys., Res., 86*, 10,049, 1981.

Swift, D. W., On the structure of the magnetic slow switch-off shock, *J. Geophys. Res., 88*, 5685, 1983.

Swift, D. W., Use of a hybrid code to model the Earth's magnetosphere, *Geophys. Res. Lett., 22*, 311, 1995.

Swift, D. W., Use of a hybrid code for a global-scale plasma simulation, *J. Comput. Phys.*, in press, 1996.

Swift, D. W., and L. C. Lee, Rotational discontinuities and the structure of the magnetopause, *J. Geophys. Res., 88*, 111, 1983.

Vasyliunas, V. M., Theoretical models of magnetic field line merging, 1, *Rev. Geophys., 13*, 303, 1975.

Vu, H. X., J. U. Brackbill, and D. Winske, Multiple switch-off slow shock solutions, *J. Geophys. Res., 97*, 13,839, 1992.

Winske, D., E. K. Stover, and S. P. Gary, The structure and evolution of slow mode shocks, *Geophys. Res. Lett., 12*, 295, 1985.

Winske, D., and N. Omidi, Electromagnetic ion/ion cyclotron instability at slow shocks, *Geophys. Res. Lett., 17*, 2297, 1990.

Yan, M., L. C. Lee, and E. R. Priest, Fast magnetic reconnection with small shock angles, *J. Geophys. Res., 97*, 8277, 1992.

Y. Lin, Department of Physics, Auburn University, 206 Allison Laboratory, Auburn, AL 36849-5311. (e-mail: ylin@physics.auburn.edu)

D. W. Swift, Geophysical Institute, University of Alaska Fairbanks, Fairbanks, AK 99775-7320.

(Received March 8, 1996; revised May 3, 1996;
accepted May 3, 1996.)